Proc. INDO-US Conference on Materials and Biological Applications 2006

PHOTOELECTRON SPECTROSCOPY OF METAL, METAL/ORGANIC, AND BIOLOGICAL CLUSTER ANIONS

W.-J.Zheng, J. M. Nilles, D. Radisic, S. T. Stokes, B. A. Trotter, S. Eustis, A. Grubisic, S. Li, and K. H. Bowen

Department of Chemistry, Johns Hopkins University, Baltimore, MD 21218, USA

INTRODUCTION

Here, we cover three topics from our work using anion photoelectron spectroscopy: (1) the electronic structure of metal clusters, (2) transition metal/ benzene anion complexes, and (3) excess electron interactions with small biomolecules. Under the first topic, we present the electronic structure studies of magnesium cluster anions. Under the second topic, we present results from our studies of Co, Fe, Ti, and Ni/benzene complexes. And under the third topic, we present work on zwitterion formation in amino acids. As a prelude to presenting specific examples of our work on these topics, we first describe the technique of Negative Ion Photoelectron Spectroscopy.

NEGATIVE ION PHOTOELECTRON SPECTROSCOPY

Negative ion photoelectron (photodetachment) spectroscopy is conducted by crossing a mass-selected beam of anions with a fixed-frequency photon beam and energy-analyzing the resultant photodetached electrons. This technique is a direct approach to measuring electron binding energies, and it is governed by the energy-conserving relationship, $h\nu = EKE + EBE$, where $h\nu$ is the photon energy, EBE is the electron binding energy, and EKE is the measured electron kinetic energy. Briefly, both mass spectra and photoelectron spectra were collected on an apparatus consisting of a laser vaporization source employing a Nd:YAG laser, a linear time-of-flight mass spectrometer for mass analysis and selection, a second Nd:YAG laser for photodetachment, and a magnetic bottle for electron energy analysis. Pure magnesium cluster anions were generated by laser vaporization (2.331 eV/photon) of a magnesium rod without the use of inert carrier gas. This resulted in homogeneous magnesium cluster anions, uncontaminated by impurities such as oxides, which had plagued previous attempts. Size-selected magnesium cluster anions were photodetached with 3.496 eV photons. The resolution of our magnetic bottle electron energy analyzer was ~60 meV at an EKE of ~1 eV.

THE TRANSITION TO METALLIC BEHAVIOR IN MAGNESIUM CLUSTERS

A collection of metal atoms does not necessarily exhibit metallic behavior. To investigate this issue, we explored the non-metallic-to-metallic transition in the finite size regime for the case of magnesium. The schematic in Figure 1 provides a simplified, yet useful framework (ignoring the presence of hydridization) for visualizing the evolving electronic structure of magnesium.

There, the energies of the most relevant orbitals are plotted versus increasing numbers of interacting magnesium atoms, n. The doubly occupied 3s energy level of the ground state atom along with the empty 3p level above it are shown on the left side of the figure. When two magnesium atoms interact to form a dimer, two molecular orbitals are formed and both are filled. As more magnesium atoms interact, new molecular orbitals are formed in like fashion, with n magnesium atoms giving n

molecular orbitals, and with these too being filled to capacity. Above these, molecular orbitals based on the 3p atomic orbitals of magnesium are also formed, but these are empty. As still more atoms interact, both the filled $3s^2$-derived molecular orbitals and the empty 3p-derived molecular orbitals broaden in energy, producing "fans" of molecular orbitals. The energy difference between the highest energy, $3s^2$-derived molecular orbital (the HOMO) and the lowest energy, 3p-derived molecular orbital (the LUMO) is the HOMO-LUMO gap, Δ, and it becomes smaller with increasing numbers of interacting magnesium atoms. Once $\Delta \rightarrow 0$, however, the filled and empty fans overlap, and electrons from the $3s^2$-derived fan of molecular orbitals spill into the fan of previously unoccupied, 3p-derived molecular orbitals, creating a partially-filled band and meeting the usual criterion for the onset of metallic behavior.

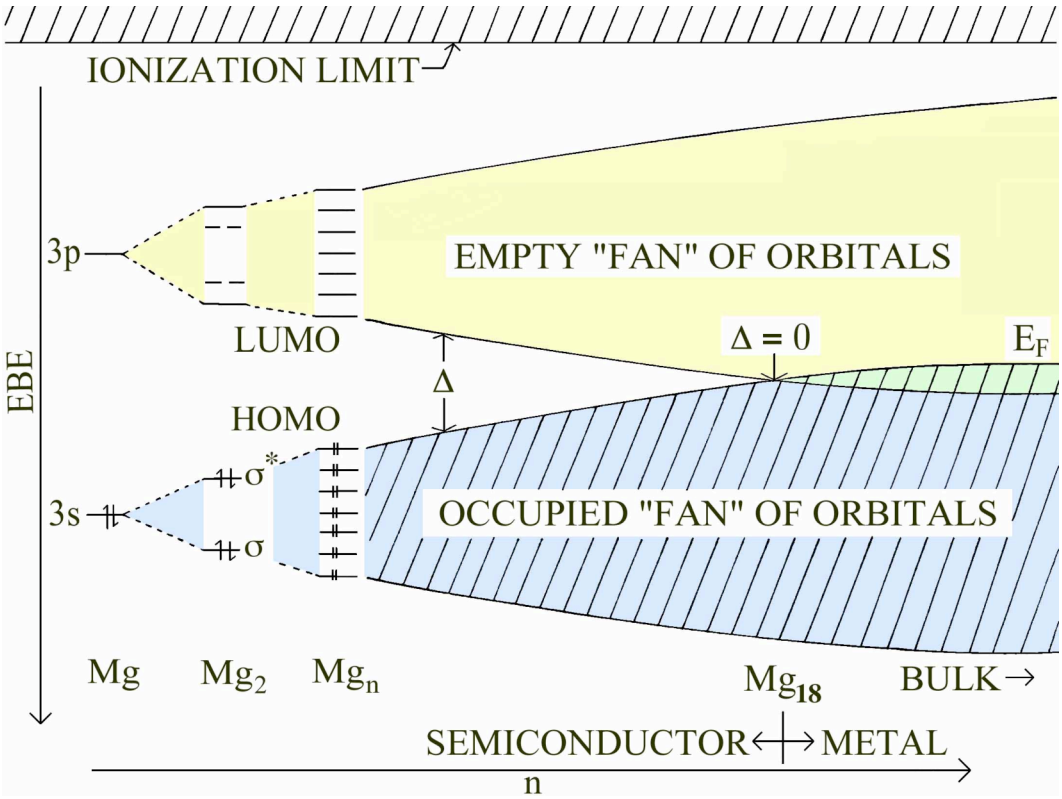

Fig. 1: Schematic of the evolving electronic structure of magnesium

Figure 1 can also be viewed as representing the evolving electronic structure of individual, neutral magnesium *clusters* as a function of size, n. If one next imagines adding an extra electron to each of these clusters to form their corresponding ground state cluster anions, then for clusters smaller than that at the gap closure, that extra electron must reside at the bottom of the previously empty, 3p-derived fan of MO's. While the energies of the MO's shown in Figure 1 as well as the gap between them are quantitatively modified by the addition of one more electron to each cluster size, the figure itself remains a qualitatively viable picture for magnesium cluster anions.

Determining the minimum number of interacting magnesium atoms at which the onset of metallicity occurs was the main objective of this work. We approached this problem, as had Cheshnovsky et al. in the case of mercury cluster anions, by photodetaching electrons from magnesium cluster anions as a function of cluster size in order to track the closure of the energy gap in the anionic system. The electron binding energy (EBE) for an electron photodetached from the bottom of the anion's singly-occupied, 3p-derived fan of MO's to the ionization limit is less than that of an electron ejected from the anion's energetically-wider and fully populated, $3s^2$-derived fan of MO's to the same ionization limit. The result is a photoelectron spectrum consisting of a single, relatively narrow peak at low electron binding energy and a broader spectral feature at higher electron binding energy. The energy separation

between them is the anion's gap and measuring it as a function of size, n, allows one to determine the cluster anion size at which it closes.

The photoelectron spectra of Mg_n^- (n=3-35, n ≠ 21) are presented in Figure 2. For n≤15, each spectrum consists of two main spectral features, in accord with the description above. The lower EBE, narrower peak corresponds to photodetachment from the bottom of the anion's 3p-derived fan, while the higher EBE, broader and sometimes structured band corresponds to electron detachment from the anion's $3s^2$-derived fan. The energy spacing between these features is a direct measure of the anion's gap. Following this spacing by eye to increasing cluster size, one observes an overall trend by which it gradually decreases, although it is also marked by "reopenings" of the gap spacing at several specific cluster sizes. For example, the spacing closes relatively smoothly from n = 3 – 9, except for a "reopening" at n = 4. The smooth closure of the gap spacing is again disrupted by the gap opening up at n = 10, only to resume its closure at n = 11 and to continue smoothly until the gap spacing disappears at n = 16. The gap spacing remains closed through n = 19, until it opens up still again at n = 20. Thereafter, the gap rapidly closes and remains closed for successive sizes through n = 34. Then, at n = 35, the gap spacing exhibits still another "reopening".

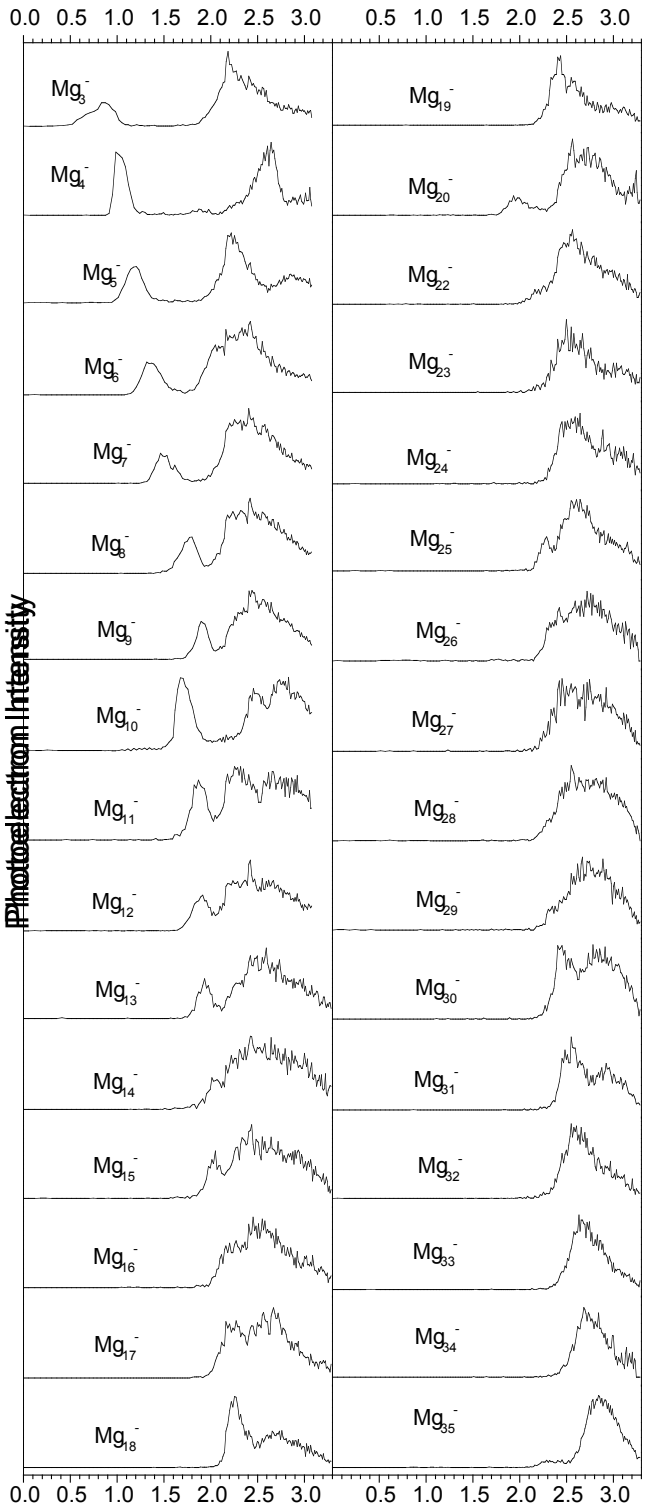

Fig. 2: Photoelectron spectra of magnesium cluster anions.

Starting at n = 16, it becomes difficult to discern a non-zero gap. So, where does the gap actually close? We assert that effective band overlap first occurs at n = 18. At this size, the gap has become comparable to kT, and this marks the onset of metallic behavior in magnesium clusters. The overlap of bands is evidenced by the dramatic change in the shape of Mg^-_{18}'s spectral profile relative to its

immediately smaller neighbors. When overlap between the orbital fans first occurs, electrons from the $3s^2$-derived fan gain access to the high density of states associated with the 3p-derived fan, giving them enhanced "p-character". This manifests itself on the low EBE side of Mg^-_{18}'s spectral profile, where the relatively sharp feature indeed resembles the shapes of 3p-derived peaks seen in larger magnesium cluster anions.

Numerical values for the gap in a given spectrum were determined by measuring the energy difference between the center of the lower EBE peak and a thermally-corrected offset point on the low EBE edge of the broad, higher EBE spectral band. Because of the source conditions used to generate these cluster anions, the photoelectron spectra are thermally broadened. The extent of broadening (both thermal and instrumental) is best gauged from the widths of the lower EBE peaks, since they represent detachment from orbitals containing only a single electron. We have used half the base width of these peaks to thermally-correct the low EBE edge of their high EBE bands. The resulting gap values are plotted as a function of cluster size in Figure 3. The underlying trend seen in this plot is the relatively smooth closing of the gap with increasing cluster size, and it is evident that the gap closes for n values in their high teens. In addition, however, this trend is also punctuated by several sudden gap "reopenings".

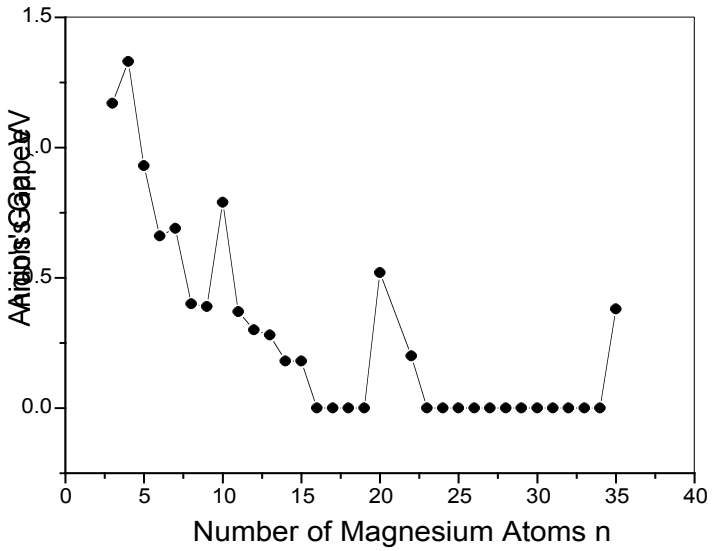

Fig. 3: Gap values vs. magnesium cluster size, n.

These "reopenings" occur at sizes, n = 4, 10, 20 and 35. For the case of a three-dimensional harmonic oscillator potential, electronic shell closings occur at 2, 8, 20, 40, 70, … valence electrons. Assuming that each magnesium atom contributes two valence electrons to a given cluster, neutral Mg_4, Mg_{10}, Mg_{20}, and Mg_{35} all meet the criterion for being closed shell species. In general, the next energy level above a closed shell level is separated from it by more energy than typically separates levels in that system. Thus, when an extra electron is added to the above closed shell neutral clusters to form anions, their photoelectron spectra reflect this "closed shell plus one electron" property by exhibiting gap "reopenings". The same effect that makes the gap unusually large necessarily minimizes the electron affinity at that same cluster size, and indeed this correlation is observed for n = 10, 20, and 35. Thus, these three "reopenings" observed in this system are clear manifestations of electronic shell model behavior.

Shell structure is even more apparent in the mass spectra of magnesium cluster anions. Figure 4 presents our mass spectrum of $Mg^-_{n=3-70}$. Dramatic maxima in ion intensity are observed for n = 4, 9, 19, 34, 46, 55, and 69, while striking minima are observed for n = 11, 21, 36, 48, and 57. This intensity profile is reproducible. The mass spectral magic numbers at n = 9, 19, and 34 are due to the same shell closings that gave rise to photoelectron spectroscopic "reopenings" at n = 10, 20, and 35. For example, Mg_9^- has 19 valence electrons, just one less than the 20 required for a shell closing. Likewise, Mg_{19}^- has 39 valence electrons, just one short of the shell closings at 40, while Mg_{34}^- has 69, just one less than 70. While magnesium cluster anions can never have an even number of valence electrons and therefore can never perfectly coincide with shell closing numbers, they do gather stability as they approach shell closures. In each case, this enhanced stability manifests itself as a local ion intensity maximum (a magic number) in the mass spectrum.

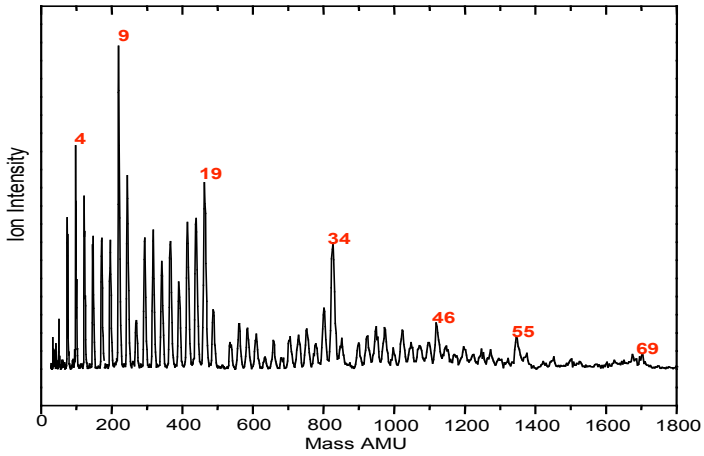

Due to the occurrence of "reopenings" and magic numbers, it is clear that the shell model plays an important role in describing the electronic structure of magnesium clusters. The situation, however, is more complex than it might appear at first sight. The applicability of the shell model has itself often been put forth as a criterion for metallic behavior. Yet, we see both a "reordering" and a magic number at n = 10 and 9, respectively, well below the observed gap closure at n = 18. Adherence to the predictions of the shell model is a working criterion for metallic behavior to the extent that it reflects electron delocalization within a finite size environment. Most likely, what we are seeing here is a hierarchy of criteria for metallic behavior, with the applicability of the shell model having some merit but with gap closure providing a somewhat stricter criterion.

TRANSITION METAL/ BENZENE ANION COMPLEXES

The interaction of metals with organic molecules is of fundamental interest to chemical and materials science. Compounds consisting of single metal atoms and multiple organic molecules are prevalent in classical organometallic and coordination chemistry, and more recently, the interaction of small metal clusters with organic molecules has become an important topic in bioinorganic chemistry. In addition, the interaction of transition metal clusters with organic substrates may soon become a significant issue in nanoscience.

Transition metal sandwich compounds, in which a metal atom lies between two parallel or nearly parallel carbocyclic ring systems, have been of interest to chemists for some time. Ferrocene and dibenzene chromium are classic examples, and the number and diversity of these compounds has grown dramatically with the recent application of gas phase synthetic strategies. An overview of recent work on organometallic compounds in the gas phase, including a review of work performed on transition metal-

benzene clusters, has been provided by Nakajima and Kaya. These investigators have explored photofragmentation processes, binding energies, structures, electron affinities, and ionization energies for various transition metal-aromatic molecule complexes.

We have studied several transition metal/organic molecule anion complexes. These include systems where the metal was cobalt, iron, titanium, and nickel. Here, we present some of our photoelectron spectroscopic results for cobalt/benzene anion complexes, along with our mass spectra for iron/benzene (Fig. 5), titanium/benzene (Fig. 6), and nickel/benzene (Fig.7) anion complexes.

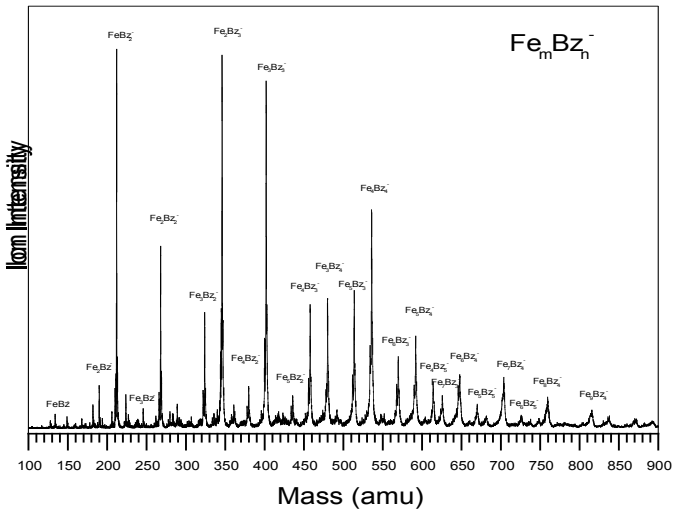

Fig. 5. Mass spectrum of iron/benzene cluster anions.

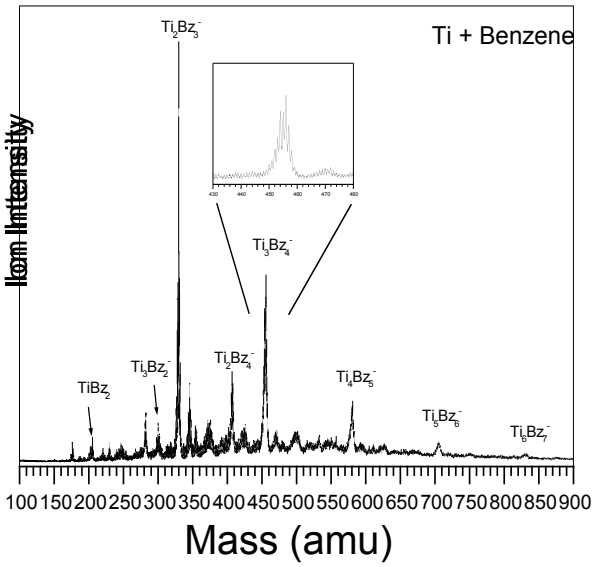

Fig. 6. Mass spectrum of titanium cluster anions.

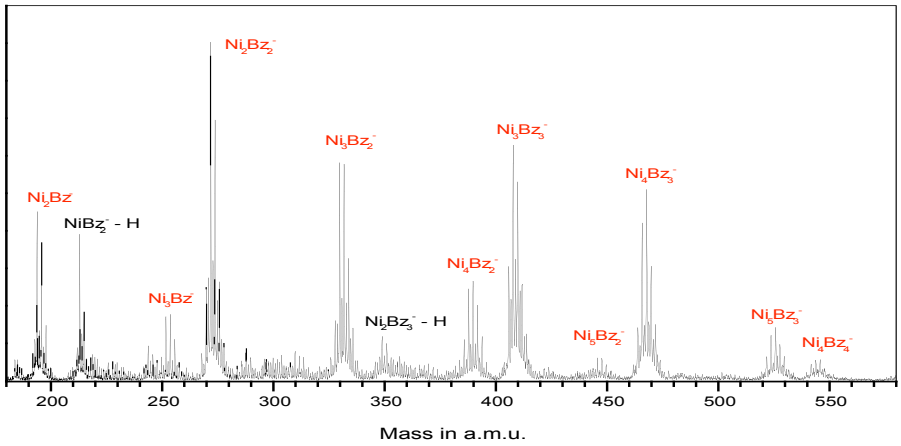

Fig. 7: Mass spectrum of nickel/benzene cluster anions.

Consider the cobalt/benzene anion complex as an example of their photoelectron spectra. In these cases, their ionization energies and mass spectral intensities have been explained in terms of two basic structural types. $Co_n(Benzene)_m$ (m = n + 1 and n = 1- 3) clusters are described as multiple-decker sandwiches, whereas $Co_n(Benzene)_m$ (n ≥ 4) form n atom metal clusters coated by m benzene molecules. The diverse structures of cobalt-benzene clusters make them attractive candidates for further study. $(Cobalt)_n(benzene)_m^-$ cluster anions, (n,m) were generated by laser vaporization and studied by both mass spectrometry and anion photoelectron spectroscopy. Our assignment of the photoelectron spectrum of the (1,2) cluster anion (see Fig. 8) suggests that it possesses a sandwich structure with the cobalt atom located between two parallel benzene rings, that the ground state of this anion is a singlet, and that the ground state of its corresponding neutral is a doublet. The photoelectron spectra of cobalt-rich cluster anions of the form, (n,1) are interpreted as cobalt metal cluster anions which have been solvent-stabilized by their interaction with, in each case, a single benzene molecule. The photoelectron spectra of the benzene-rich cluster anions, (2,3), (2,2), and (3,3) are tentatively interpreted as suggesting extended sandwich structures for these anion complexes.

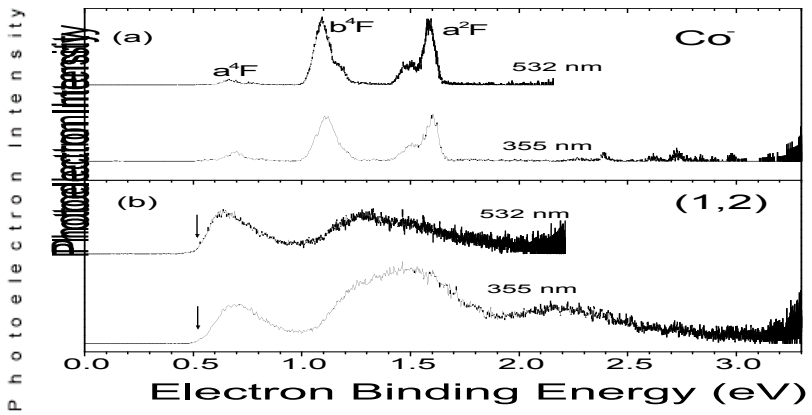

Fug. 8: Photoelectron spectra of the Co^- atomic anion and the $cobalt(benzene)_2^-$ cluster anion.

EXCESS ELECTRON INTERACTIONS WITH SMALL BIOMOLECULES

The hydration of biological molecules ranks among the most important problems in biology. At the macroscopic level, seasonal changes in biological phenomena are often triggered by the availability of water. While the naturally-occurring amino acids are not zwitterions in the vapor phase, they are in

aqueous solutions, implying that water plays an important role in inducing zwitterion formation. Together, these observations inspire the question, "How many water molecules are required to induce zwitterion formation in a given amino acid molecule?" We have addressed this question in the context of mass spectrometric and size-selected photoelectron spectroscopic studies of hydrated amino acid anions. We utilized the facts that zwitterions possess very large dipole moments, and that excess electrons can bind to strong dipole fields to form dipole bound anions, which in turn display distinctive and recognizible photoelectron spectral signatures. The appearance of dipole-bound photoelectron spectra of hydrated amino acid anions, beginning at a given hydration number, thus signals the onset of greatly enhanced dipole moments there and, by implication, of zwitterion formation. We find that five water molecules are needed to transform glycine into its zwitterion, while four each are required for phenylalanine and tryptophan.

Figure 9 shows our photoelectron spectra of glycine/water cluster anions, while Figure 10 shows examples of other photoelectron spectra of dipole bound anions that we have studied.

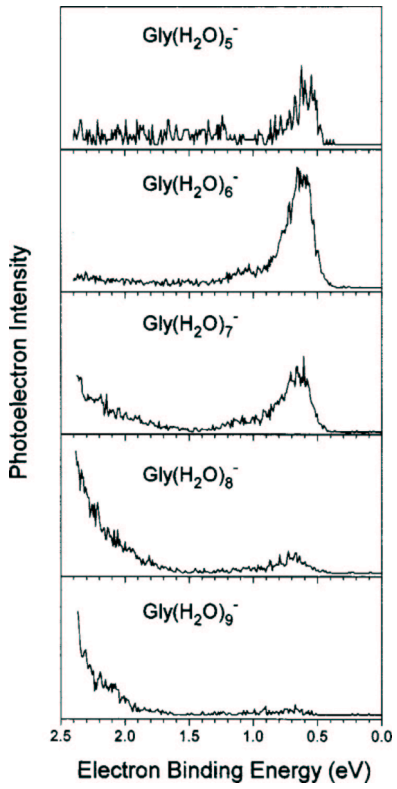

Fig. 9

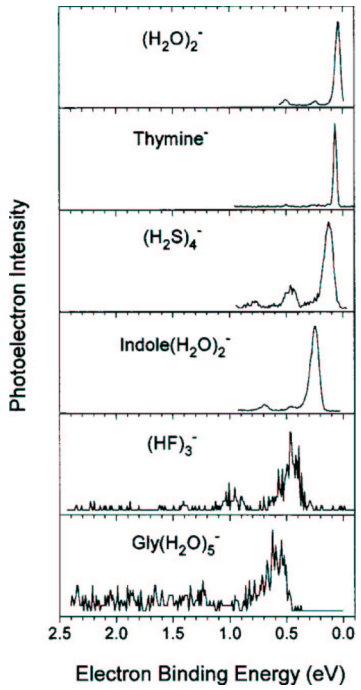

Fig. 10

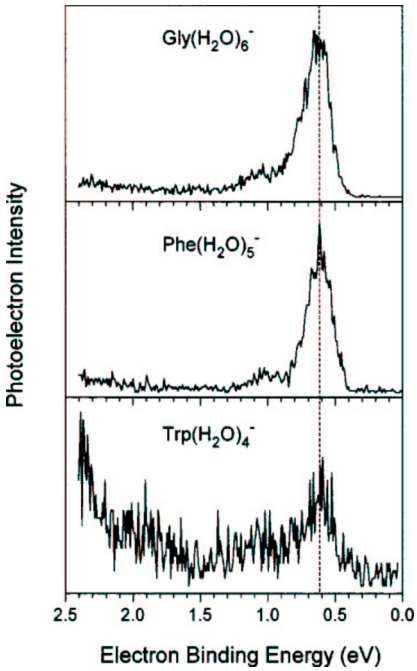

Fig. 11

Fig. 9: Photoelectron spectra of glycine(water)$_n^-$ cluster anions.

Fig. 10: Examples of photoelectron spectra of dipole bound anions.

Fig. 11: A comparison of representative photoelectron spectra of hydrated glycine, phenylalanine, and tryptophan anions.

Figure 11 shows the photoelectron spectra of typical members of the hydrated glycine, phenylalanine, and tryptophan anions. Notice that they all occur at the same electron binding energies. This is because all three of these amino acids are structurally similar at their zwitterion-forming ends. This is further evidence that these spectra derive from electron attachment to the charge-separated, zwitterion portion of these amino acids.

ACKNOWLEDGMENT

This work was supported by The US National Science Foundation (zwitterions), the US Departmnt of Energy (magnesium and transition metal/organic anion complexes), and the Petroleum Research Foundation (metal/organic anion complexes).